CHEMICAL ENGINEERING TRANSACTIONS Volume 21, 2010
Editor J. J. Klemeš, H. L. Lam, P. S. Varbanov
 ISBN 978-88-95608-05-1 ISSN 1974-9791
DOI: 10.3303/CET1021024

Exergy analysis of an isothermal heat pump dryer

William Catton*, Zhifa Sun, Gerald Carrington
Department of Physics, University of Otago, 730 Cumberland St, Dunedin 9016, New Zealand
wcatton@physics.otago.ac.nz

We determine the energy efficiency benefit obtainable from an isothermal plate-type heat pump dryer employing contact heat transfer, by developing a numerical simulation to compare such a system with a conventional heat pump dryer. The model presented combines a comprehensive heat pump model with a detailed air-flow model, which solves the mass, momentum and energy balances within the drier ducts. We assess the accuracy of an idealised model used in a previous analysis. Although the performance of the idealised model is sensitive to system temperature variations, this does not lead to significant error under typical heat pump drying conditions. We employ exergy analysis to examine the benefit associated with contact heat pump drying. Isothermal drying is found to reduce irreversibility occurring within the refrigerant cycle by roughly the same amount as that occurring in heat transfer from the condenser to the product.

1. Introduction

The present work centres on a simple idea for increasing the energy efficiency of heat pump driers (Carrington and Scharpf, 2004). The idea arises naturally from consideration of the Gouy-Stodola law (Bejan, 1997). In a conventional adiabatic heat pump drying (HPD) system, recycled heat is returned to the drying process by heating the dehumidified airstream as it re-approaches the product. But from a second-law viewpoint, this approach – using air for heat transfer – appears wasteful. Heat transfer to the air, and from the air to the drying process, is responsible for a substantial part of the entropy creation in such a system; so are losses owing to the airflow resistance of the system, and fan friction. The idea behind the present work is that these irreversibilities can be reduced by providing heat directly to the drying process, through a conductive plate separating the refrigerant and the product (plates labelled CD2 in Figure 1) – an instance of the broad process integration philosophy discussed by Friedler (2009). Such a system would be most applicable to the drying of products that can be spread into thin layers, especially those that can be dried under high-humidity conditions. Two examples of potential applications for isothermal HPD are: (1) high-energy-efficiency, emission-free drying of industrial sludges, reducing costs associated with transport and land-filling (Macolino et al., 2009); (2) high-energy-efficiency drying of biofuel feedstock (Ehiaze et al., 2009). The system depicted in Figure 1 becomes equivalent to a standard (adiabatic) HPD if the refrigerant bypasses the plates (dotted line 2-2').

Please cite this article as: Catton W. R., Sun Z. F. and Carrington C. G., (2010), Exergy analysis of an isothermal heat pump dryer, Chemical Engineering Transactions, 21, 139-144 DOI: 10.3303/CET1021024

A preliminary performance assessment of such a system has been performed previously, and has indicated energy performance benefits of 2-3 times compared with an adiabatic HPD (Catton et al., 2010). However, this analysis was based on a highly idealised system model. The heat pump heating COP was assumed to be a constant percentage (50%) of the Carnot COP. Also in the isothermal (contact) case the model assumed that the temperatures of the product surface (T_s) and of the bulk air (T_b) were everywhere equal to that at the drier inlet (i.e. location *D* in Figure 1). Thus although the analysis was able to satisfactorily match measured data in the adiabatic case, substantial uncertainty remained, particularly in its predictions for the isothermal mode. The present work extends the previous analysis by incorporating a detailed model of the drying process occurring within the drier ducts. In addition a detailed model of the refrigerant system is included. We present results from the resulting system model, including a second-law analysis comparing the adiabatic and isothermal modes.

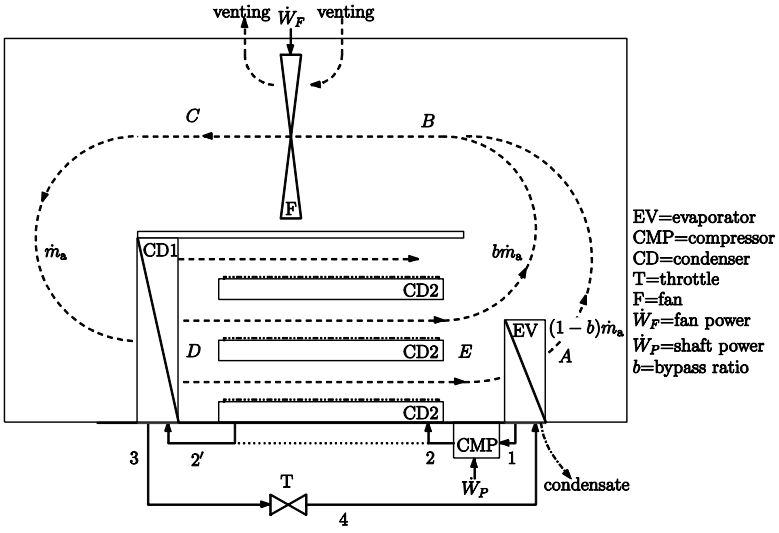

Figure 1: Schematic of heat pump drying system being modeled. The system geometry is as specified by Catton et al. (2010).

2. Theory

The idealised drier model was based on the following expression for the drier outlet humidity ratio ω_E, using the isothermal assumption $T_s = T_D$ or the adiabatic assumption $T_s = T_{wb,D}$, i.e. T_s given by the wet-bulb temperature of the inlet air (Catton et al., 2010):

$$\omega_E = \omega_{sat}(T_s) + [\omega_D - \omega_{sat}(T_s)] \exp\left(-\frac{h_m \rho_a N_D w}{\dot{m}_a} L\right) \quad (1)$$

Here we briefly describe the detailed drier model. The time-averaged control-volume mass, momentum and energy balance equations are solved in a 1-D plug-flow model of a drier duct (between locations *D* and *E* in Figure 1), using the SIMPLER algorithm described by Patankar (1981), subject to the inlet air flow velocity and psychrometric

state, the outlet pressure p_E, the refrigerant saturated condensing temperature, and standard transfer correlations for duct flow, adjusted for high mass transfer rates (Bird et al., 1960). Only the constant drying-rate period is considered. The product surface temperature T_s for each control-volume is evaluated by solving the energy balance at this surface (Catton et al., 2010, Keey, 1978, p.222). The adiabatic mode can be simulated by setting the plate thermal conductivity to zero. To allow comparison with the previous analysis, the top surface of each duct is assumed to be adiabatic.

In addition to the detailed dryer model described above, the system model used in the present work incorporates the isentropic and volumetric efficiencies of the ZR61K2-TFD scroll compressor with R134a characterised by Carrington et al. (1996). The whole-system model uses an approach similar to that described by Goldstein (1983) and by Carrington and Bannister (1996). The Newton-Raphson method is applied to the state vector $\boldsymbol{x} = (T_{rsat1}, T_{rsat3}, \omega_D)$. Using the compressor model and assuming isenthalpic throttling, the two saturated refrigerant states T_{rsat1} and T_{rsat3} are sufficient to specify the refrigerant thermodynamic cycle (where 5°C of subcooling and of superheating is assumed) and mass flow rate m_r. A constant fan efficiency of 50% is assumed. The pressure at location E is set equal to ambient: p_E =101325 Pa. The pressure drop within the drier is evaluated using the SIMPLER algorithm; other air pressure drops are estimated using the dynamic loss coefficients (k-factors) specified by Carrington et al. (2000). Venting is controlled to maintain T_D fixed. Thus the air state at location D is specified by ω_D, p_D. Air states around the system are obtained using the drier model and energy balances across the HP components. The error vector $\boldsymbol{\Delta}$ used in the Newton-Raphson method is specified as: $\Delta_1 = m_r(h_1 - h_4) - f_{ev}(v_{ev}, T_{wb,E}, T_4)$; $\Delta_2 = m_r(h_{2'}-h_3) - f_{co}(v_{co}, T_C, T_{rsat,3})$; $\Delta_3 = \omega_D - \omega_C$, where f_{ev} and f_{co} are specified by equations (4) and (7) of Carrington and Bannister (1996). These functions are empirical component heat transfer correlations based on the incoming flows.

3. Results and discussion

An example output of the detailed air-flow model, shown in Figure 2, can be seen to compare favourably with the idealised model. Here air enters at state T_D=55°C and ω_D=0.031 kg/kg-dry, at a dry air mass flow rate of 1 kgs^{-1} into a stack of N_D=10 ducts, width w=1m, presenting a total face area of 0.2m^2. The refrigerant saturated condensing temperature is 60°C. Fifty duct control-volumes are used; no significant difference is detected at greater numbers of control-volumes. The detailed model incorporates a number of physical effects not accounted for in the idealised model. The most important, which is visible in Figure 2, is that the product surface and bulk air temperatures may vary substantially from their idealised values. At moderate drying rates the idealised and detailed models are in good agreement; however at very high and very low drying rates, correspondingly depressed and elevated surface temperatures (respectively) may have a substantial effect on evaporation within the dryer, as is illustrated in Table 1. When the product surface temperature is forced equal to T_D in the detailed model, the result is near-agreement (to within 4% for the scenarios shown in Table 1) with the moisture extraction rate (MER) predicted by the idealised model. These results indicate (1) that the idealised model provides a reasonable first-order approximation; (2) that the detailed model may be required in order to describe

significant temperature effects at low and high drying rates; and (3) that the other additional physical effects included can be regarded as corrections, rather than as primary aspects of the situation being modelled.

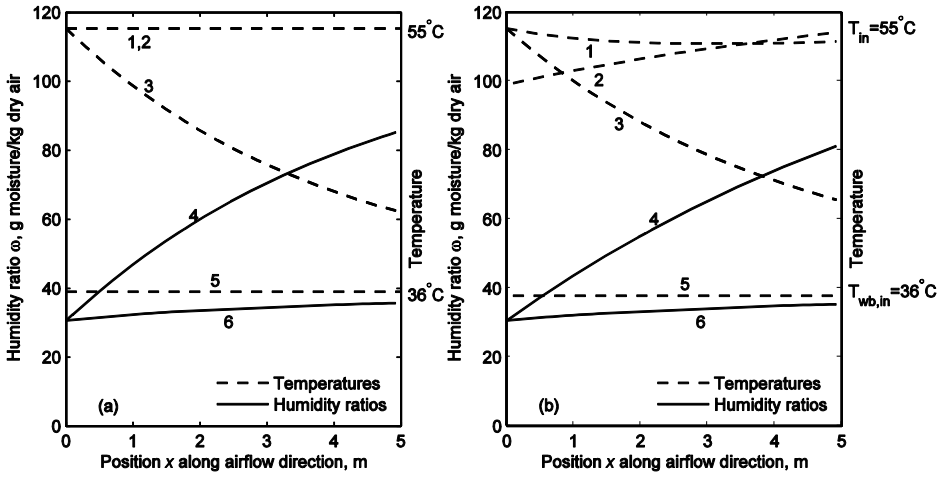

Figure 2: Example profiles (from D to E) (a) idealised model, (b) detailed model. 1: T_b (ISO). 2: Ts (ISO). 3: T_b (ADI). 4: ω (ISO). 5: Ts (ADI). 6: ω (ADI).

Table 1. Estimates of system behaviour.

		Idealised model	Detailed model
ISO	φ_{in}=30%	MER=199.3 kg/h	MER=179.8 kg/h
	T_{in}=55°C	T_{out}=55.0°C	T_{out}=54.0°C
ADI	φ_{in}=30%	MER=21.2 kg/h	MER=19.2 kg/h
	T_{in}=55°C	T_{out}=41.8°C	T_{out}=42.5°C
ISO	φ_{in}=60%	MER=50.4 kg/h	MER=67.3 kg/h
	T_{in}=40°C	T_{out}=40.0°C	T_{out}=41.6°C
ISO	φ_{in}=60%	MER=122.6 kg/h	MER=127.2 kg/h
	T_{in}=55°C	T_{out}=55.0°C	T_{out}=55.3°C
ISO	φ_{in}=90%	MER=33.1 kg/h	MER=70.6 kg/h
	T_{in}=55°C	T_{out}=55.0°C	T_{out}=56.6°C
ISO	φ_{in}=60%	MER=314.7 kg/h	MER=218.1 kg/h
	T_{in}=70°C	T_{out}=70.0°C	T_{out}=68.2°C

We now consider an illustrative output from the detailed whole-system model. Figure 3 shows the refrigerant cycle under typical isothermal and adiabatic HPD conditions. The two modes have identical system specifications aside from plate heat transfer. T_D=55°C; evaporator bypass ratio b=0. Isothermal operation is seen to allow the system to operate over a significantly smaller temperature range, enhancing the COP of the heat pump. The resulting MERs and specific moisture extraction rates (SMERs) are: MER_{iso}=58.3

kg/h; MER_{adi}=25.0 kg/h; $SMER_{iso}$=14.8 kg/kWh; $SMER_{adi}$=4.6 kg/kWh. (Under the idealised isothermal assumption, the results would be MER_{iso}=57.0 kg/kWh, $SMER_{iso}$=14.6 kg/kWh.) Table 2 shows the exergy destroyed per kg moisture removed from the product in key system processes and components. In evaluating the exergies (and venting), the environment has been taken to be saturated at 10°C. Noteworthy features of the data are: (1) In the adiabatic mode, condenser and product irreversibilities contribute much of the overall work requirement; (2) The isothermal mode greatly reduces this irreversibility, by about ten-fold per kg moisture removed; (3) A significant part of the overall reduction of irreversibility nevertheless takes place in the compressor and the throttle. This last result highlights the synergistic nature of a heat pump dryer, and implies that the exergy destruction in the condenser and product of an adiabatic HPD does not set an upper bound on the SMER gain associated with isothermal HPD. (Indeed if it did, the isothermal SMER could not exceed 7.6 kg/kWh.)

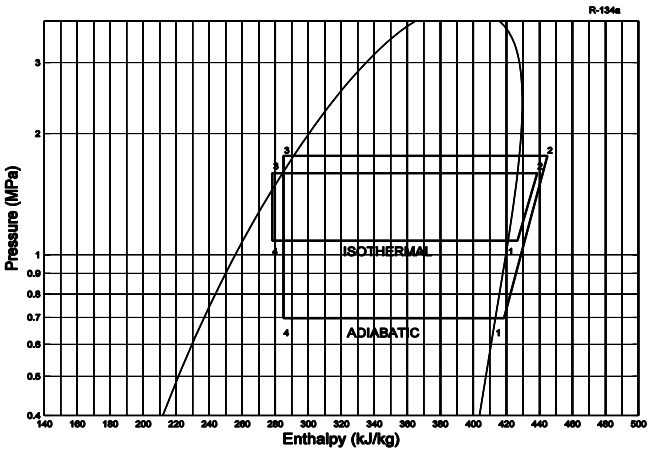

Figure 3. Thermodynamic cycle of R134a in the isothermal and adiabatic modes.

Table 2. Specific exergy destruction by component.

($\times 10^{-3}$), kWh/kg	Adiabatic HPD	Isothermal HPD
Condenser and product	85.0	8.2
Compressor	54.3	20.1
Evaporator	25.7	21.4
Throttle	33.1	10.1
Fan friction	4.3	2.4
Venting and condensate	13.3	5.2

4. Conclusions

A detailed model of an isothermal heat pump drier has been developed, which solves the mass, momentum and energy balances for the air flow within the drier ducts. This detailed model has been used to show that the assumption of purely isothermal

conditions within a contact heat pump drier is the most severe restriction applying to the idealised model previously used in an analysis of contact HPD. Other assumptions have been shown to make a much smaller difference to model predictions. A whole-system HPD model has been produced by combining the detailed air flow model with models of the remaining heat pump components. This whole-system model has been used to confirm the previous finding that isothermal contact dehumidification drying may increase drying energy efficiency by 2-3 times compared with conventional adiabatic dehumidification HPDs. The deviation from purely isothermal behaviour has been found to influence the MER and SMER that is predicted by the whole-system model by only a few per cent. An exergy analysis of the system has been performed for both the isothermal and adiabatic modes, and this has provided explanation for the observed energy efficiency gain. The analysis has shown that the promised energy performance benefit of isothermal HPD results partially, but by no means entirely, from a relative reduction in the irreversibility associated with the transfer of heat to the drying process. By narrowing the HP temperature range, the isothermal mode also yields substantial reductions in irreversibility mechanisms that occur within the refrigerant cycle.

References

Bejan, A. (1997). Advanced Engineering Thermodynamics, Second Edition. JohnWiley.

Bird, R., Stewart, W., and Lightfoot, E. (1960). Transport Phenomena. Wiley, New York.

Carrington, G. and Bannister, P. (1996). An empirical model for a heat pump dehumidifier drier. International Journal of Energy Research, 20:853–869.

Carrington, G., Bannister, P., and Liu, Q. (1996). Performance of a scroll compressor with R134a at medium temperature heat pump conditions. International Journal of Energy Research, 20:733–743.

Carrington, G. and Scharpf, E. (2004). Dehumidifier drier for pastes, liquors and aggregate materials. NZ Patent 526648.

Carrington, G., Sun, Z., Sun, Q., Bannister, P., and Chen, G. (2000). Optimizing efficiency and productivity of a dehumidifier batch dryer. Part 1: capacity and airflow. International Journal of Energy Research, 24:187–204.

Catton,W., Carrington, G., and Sun, Z. (2010). Performance assessment of contact heat pump drying. International Journal of Energy Research. doi: 10.1002/er. 1704.

Ehiaze, E., Sun, Z., and Carrington, G. (2010). Variables affecting the in situ transesterification of microalgae lipid. Fuel, 89(3):677–684.

Friedler, F. (2009). Process integration, modelling and optimisation for energy saving and pollution reduction. Chemical Engineering Transactions, 18, 1-26.

Goldstein, S. (1983). Simulation parameters and methods of finding equilibrium statepoints in refrigerant systems. ASHRAE Trans. Part 2A, 89:436–446.

Keey, R. (1978). Introduction to Industrial Drying Operations. Pergamon Press.

Macolino P., Bianco B., Veglio F. (2009) Drying process of a biological industrial sludge: Experimental and process analysis. Chemical Engineering Transactions, 17, 699-704.

Patankar, S. (1981). Numerical Heat Transfer and Fluid Flow. McGraw-Hill Book Company, New York.